Structural and electronic stability of a volleyball-shaped B_{80} fullerene

Xiao-Qian Wang

Department of Physics and Center for Functional Nanoscale Materials, Clark Atlanta University, Atlanta, Georgia 30314, USA

We have studied the structural and electronic characteristics of a volleyball-shaped B_{80} cage using first-principles density-functional calculations. In contrast to the popularly ratified "magic" B_{80} buckyball with 20 hexagonal pyramids and 12 hollow pentagons, the volleyball-shaped B_{80} constitutes 12 pentagonal pyramids, 8 hexagonal pyramids, and 12 hollow hexagons. The B_{80} volleyball is markedly more stable than the previously assumed magic B_{80} buckyball, which is attributed to the improved aromaticity associated with the distinct configuration.

Boron is an electron-deficient element that has an intriguing versatility in chemical bonding. A combination of two and three center bonding, along with hybrid covalent and metallic characters, yields a remarkably rich class of pure boron nanostructures, including clusters, rings, cages, and nanotubes.[1–4] Recent theoretical work by Szwacki *et al.*[1] predicted a highly stable B_{80} cage. The boron buckyball B_{80} is structurally analogous to the celebrated C_{60},[5] with 60 boron atoms located at the vertices of a truncated icosahedron consisting of 12 pentagons and 20 hexagons, reinforced by extra 20 boron atoms placed in the center of each hexagon. The addition of 20 capping atoms stabilizes the cage, which has the same icosahedral (I_h) symmetry as the C_{60} buckyball.

The architectural magnificence and the predicted high stability of this boron buckyball have prompted a flurry of efforts in designing B_{80}-related nanomaterials such as endohedral complexes,[6] solids,[7,8] and hydrogen-storage media.[9] The chemical-bonding pattern of B_{80} sheds pivotal insights into the nature of boron nanomaterials. Inspired by the B_{80} buckyball configuration [cf. Fig. 1(a)] with an appealing interplay of two- and three-center bonds, guidelines for constructing a family of stable boron fullerenes were suggested.[10] Moreover, the chemical bonding of B_{80} buckyball with triangular and hexagonal motifs led to closer scrutiny of conventionally assumed structures of boron sheets and nanotubes comprised of solely puckered triangular motifs, resulting in the discovery of more stable α-boron sheet[11] along with the associated boron nanotubes and nanoribbons.[12]

While the "magic" boron buckyball is generally believed to be the most stable conformation among 80-atom boron clusters, its relative stability with respect to alternative structural conformations is subject to open debate. Specifically, *ab initio* calculations revealed a vibrational instability of the I_h boron buckyball, and suggested a slightly puckered cage with tetrahedral (T_h) symmetry [cf. Fig. 1(b)].[13–16] Subsequent investigations[13] indicated that the atomic buckling is particularly sensitive to the basis set employed and the level of theory used in describing exchange-correlation effects. Accurate *ab initio* calculations[14–16] demonstrated that the energy difference between the two configurations is very small (typically less than 0.03 eV) whereas large-scale *ab initio* calculations up to second-order Møller-Plesset perturbation theory reinstalled the I_h boron buckyball as the lowest energy conformation.[13] Nevertheless, the electronic properties of

B_{80} buckyball closely resemble those of C_{60} in that each has a total of 240 electrons, and the lowest unoccupied molecular orbital (LUMO) is triply degenerate.

On the other hand, recent *ab initio* simulation studies uncovered a few lower energy (more than 2 eV) structures built by an icosahedral B_{12} core along with a shell of pentagonal and hexagonal pyramidal units.[17,18] The core-shell structures can be regarded as fragments of boron solids. Notwithstanding the fact that the core-shell B_{80} structures [cf. Fig. 1(c)] possess no descriptive symmetry and apparently squander the connection to C_{60}, this adds new wrinkle to the debate regarding the stability of boron cages.

Herein we report on yet another volleyball-shaped B_{80} cage [cf. Fig. 1(d)] that has even lower energy than the core-shell-structured B_{80} while preserves the desired electronic properties as the boron counterpart of C_{60}. The B_{80} volleyball constitutes 12 pentagonal pyramids, 8 hexagonal pyramids, and 12 hexagon rings, in contrast to the magic boron buckyball (with either I_h or T_h symmetry) consisting of 12 pentagon rings and 20 hexagonal pyramids. Our findings not only assert the stability of boron cage structures but also pinpoint the route for building highly stable boron cages.

(a) I_h (0 eV)   (b) T_h (-0.0 eV)

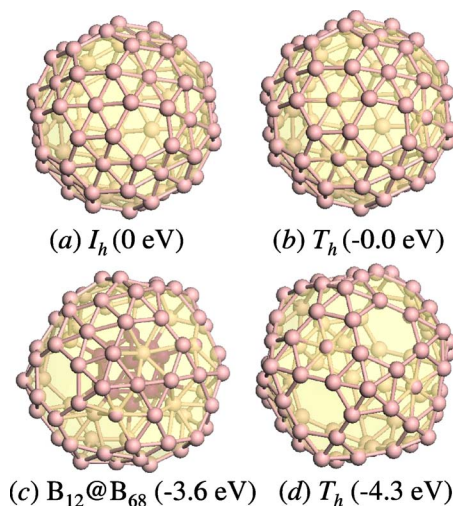(c) $B_{12}@B_{68}$ (-3.6 eV)   (d) T_h (-4.3 eV)

FIG. 1. (Color online) Optimized structures of (a) the magic boron buckyball of I_h symmetry, (b) a slightly puckered cage of T_h symmetry, (c) the core-shell-structured $B_{12}@B_{68}$, and (d) the B_{80} volleyball, respectively.

TABLE I. Calculated energy ΔE relative to the I_h boron buckyball, the symmetry of HOMO ($\mathcal{S}_H$) and LUMO ($\mathcal{S}_L$), and HOMO-LUMO gap (E_g) for the B_{80} buckyballs (I_h, T_h-A, and T_h-B), the core-shell-structured $B_{12}@B_{68}$, and the B_{80} volleyball, respectively.

Structure	Method	ΔE (eV)	$\mathcal{S}_H$	$\mathcal{S}_L$	E_g (eV)
I_h	BLYP, DNP	0	h_u	t_{1u}	1.01
T_h-A	BLYP, DNP	−0.01	t_u	t_u	1.03
T_h-B	BLYP, DNP	−0.00	e_u	t_u	0.94
$B_{12}@B_{68}$	BLYP, DNP	−1.46	a_u	a_u	0.38
Volleyball	BLYP, DNP	−2.00	t_u	t_u	0.27
I_h	B3LYP, 6-311G	0	h_u	t_{1u}	1.87
T_h-A	B3LYP, 6-311G	−0.03	t_u	t_u	1.84
T_h-B	B3LYP, 6-311G	−0.01	e_u	t_u	1.70
$B_{12}@B_{68}$	B3LYP, 6-311G	−3.60	a_u	a_u	1.10
Volleyball	B3LYP, 6-311G	−4.32	t_u	t_u	0.86

Our first-principles calculations were based on local and semilocal density-functional approach. For prescreening structural conformations, geometry optimizations, and vibrational calculations, gradient-corrected Becke-Lee-Yang-Parr (BLYP) parametrization[19,20] of the exchange correlation was used along with double numerical (DN) or double numerical plus polarization (DNP) basis sets as implemented in the DMOL$_3$ package.[21] The local-density-functional calculation results were subsequently rectified through semilocal approach using Becke-3-parameter-Lee-Yang-Parr (B3LYP) for exchange-correlation functional,[19,20] with 6-311G or 6-311++G basis sets as implemented in the TERACHEM package.[22] The optimization of atomic positions was performed for local and semilocal calculations, which proceeded until the forces were less than 0.01 eV/Å and the change in energy was less than 3×10^{-4} eV.

Stable boron conformations can be constructed on the basis of two basic building blocks—the pentagonal pyramid B_6 and the hexagonal pyramid B_7, which is referred to as the "Aufbau principle."[23] The hexagonal B_7 is the precursor for convex and quasiplanar boron clusters and is thus closely connected to the α-boron sheet or boron nanotubes.[11] The pentagonal B_6 unit is typically viewed as the building block of stable bulk boron. However, it is worth noting that the B_6 pyramid manifests itself as an aromatic component in planar boron clusters such as B_{19}^-.[2]

Illustrated in Fig. 1 are the optimized structures of the boron buckyball [Figs. 1(a) and 1(b) for I_h and T_h symmetry, respectively], the core-shell-structured $B_{12}@B_{68}$ [Fig. 1(c)], and the volleyball-shaped B_{80} [Fig. 1(d)]. The T_h symmetry group is the highest subgroup of I_h. The characteristic feature of the T_h distortion from the I_h boron buckyball is a concerted motion of capping atoms. In accordance with the T_h symmetry, the T_h-A (T_h-B) configuration of the boron buckyball has eight boron atoms in the centers of hexagonal rings moving inward (outward) toward the center of the cage while the other 12 moving outward (inward).[14–16] The B_{80} volleyball identified in the present work can be viewed as the 12 outward capping atoms in T_h-A migrating from hexagonal pyramids to the centers of 12 empty pentagons. The ex-

change between B_6 and B_7 pyramids, along with the associated switching between empty pentagons and hexagons, suggests an alternative way of wrapping a boron sheet into the B_{80} volleyball. The core-shell coordinates were extracted from published results,[18] followed by full structural relaxations. Careful examination of the optimized core-shell $B_{12}@B_{68}$ structure reveals that there are pentagonal pyramids and empty hexagons as well.

The rearrangement among pentagonal and hexagonal rings and pyramids has a great impact on the structural stability. We summarized in Table I the calculation results of relative energies and gaps between the highest occupied molecular orbital (HOMO) and LUMO for the B_{80} configurations shown in Fig. 1. As is readily observable from Table I, both $B_{12}@B_{68}$ and the B_{80} volleyball is much lower in energy than the previously assumed magic B_{80} buckyball. The new T_h-structured B_{80} fullerene is the most stable structure. Since the T_h conformation has the shape of a volleyball, we refer the new B_{80} fullerene as volleyball B_{80}. The local and semilocal density-functional results yield equivalent energy order and trend for HOMO-LUMO gap, which are in conformity with corresponding results in the literature.[13–17] However, it is worth noting that the semilocal corrections are substantial. At the B3LYP level of theory and 6-311G basis set, the energy improvement of the B_{80} volleyball over the I_h boron buckyball is 4.32 eV, and the ensuing HOMO-LUMO gap is 0.86 eV. The convergence of these results was verified using 6-311++G basis set. It is worth pointing out that although our results indicate important cancellation of various exchange and correlation effects, the energy difference between the buckyball and volleyball B_{80} is so large that there is no ambiguity for our conclusions. This is to be contacted to the case of energy differences between I_h-B_{80} and slightly puckered T_h-B_{80}, in which highly accurate calculations are necessary for the clarification.[13]

The optimized B_{80} volleyball also shows attendant displacements of capping atoms with 12 outward and eight inward capping atoms in the centers of pentagon and hexagon pyramids, respectively. By way of contrast to the B_{80} buckyball in which there exist two distinct configurations (T_h-A
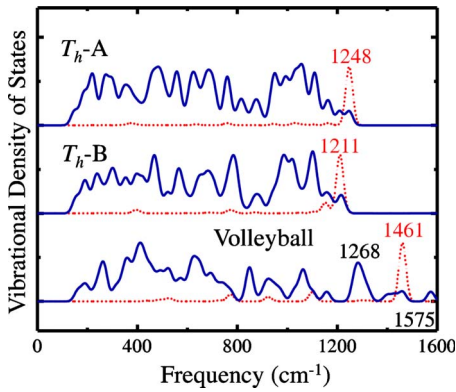
FIG. 2. (Color online) Calculated vibrational density of states (blue solid lines) and the infrared spectrum (red dotted lines) for B_{80} buckyballs (T_h-A and T_h-B), and the B_{80} volleyball, respectively. The calculation was based on local-density-functional BLYP approach and DN basis with a Gaussian broadening of 20 cm^{-1}.

and T_h-B) with concerted displacements, the oppositely displaced capping conformation is not stable against the optimal B_{80} volleyball after structural relaxation. Geometry optimization without symmetry constraint confirmed that the new B_{80} cage has the T_h symmetry. The B_{80} volleyball has five inequivalent atoms whose positions in angstrom are (1.4494, 3.6629, −1.7178), (−2.1760, 2.1760, 2.1760), (−0.9116, 2.7839, −3.1706), (0.8421, 1.3626, 0.0000), and (0.0000, 4.0926, 0.7950). The coordinates of remaining atoms can be extracted using symmetry operations of T_h.

The unique structural feature of the B_{80} volleyball is also manifested in the vibrational frequencies. We depict in Fig. 2 the calculated vibrational density of states along with infrared (IR) spectra for the B_{80} volleyball. The calculated vibrational frequencies are all real and thus the stability of the B_{80} volleyball is substantiated. In comparison with the vibrational spectra of the buckyball, the volleyball spectra indicate overall blueshift of the vibrational frequencies. For instance, the lowest Raman active mode is at 160 cm^{-1} and 152 cm^{-1} for volleyball and T_h-B buckyball, respectively. The corresponding dominant IR-active peak is at 1461 vs 1211 cm^{-1}. This implies that the out-of-plane lifting of the cap atoms in the centers of pentagonal pyramids is substantially stable than those in hexagonal pyramids. The B_{80} volleyball also has significant IR peaks at 522, 534, 726, 772, 923, 1101, and 1323 cm^{-1}. The Raman spectrum shows a wide distribution of frequencies ranging from 160 to 1575 cm^{-1}.

We are now in a position to describe the electronic characteristics. For the I_h boron buckyball, the HOMO is a fivefold degenerate h_u level and the LUMO is the triply degenerate t_{1u} one, which is identical to C_{60}. The h_u symmetry of I_h for HOMO splits into a triply degenerate t_u and a doubly degenerate e_u level in the T_h structure. The HOMO for the T_h volleyball and T_h-A has t_u symmetry while that for T_h-B is of e_u symmetry. It appears that the displacement pattern of capping atoms in the T_h is correlated with the symmetry of HOMO. On the other hand, the LUMO is triply degenerate for B_{80} volleyball and buckyballs, which is reminiscent of the LUMO orbital degeneracy of C_{60} and suggests similar metallic and even superconducting properties upon doping.
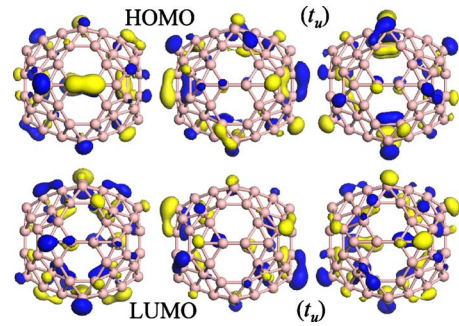

FIG. 3. (Color online) Isodensity surfaces (the isovalue is 0.02 a.u.) of triply degenerate HOMO and LUMO for the B_{80} volleyball.

Shown in Fig. 3 are the calculated charge-density distribution of HOMO and LUMO for the B_{80} volleyball. A distinctive feature of the charge-density distribution of HOMO (LUMO) is an evident decrease in the $\sigma(\sigma^*)$ bonding and an increase in the $\pi(\pi^*)$ bonding in the B_{80} volleyball, as compared to that for B_{80} buckyballs.[1] This is attributed to the redistribution of the bonding and antibonding patterns related to the capping of pentagon rings in the B_{80} volleyball. For B_{80} buckyballs, the HOMO (LUMO) has alternative bonding and antibonding (antibonding and bonding) for hexagon-hexagon and pentagon-hexagon bonds, respectively. The center of the pentagon ring displays a predominant negative electrostatic potential distribution. In contrast, the corresponding negative electrostatic potential distribution in the B_{80} volleyball moves to the isolated hollow hexagon pair region. The resultant charge distribution is thus smoother due to the expanded "empty" domain of hollow hexagon pairs. As such, the striking stability of the B_{80} volleyball can be attributed to the highly improved aromaticity associated with the rearrangement of boron atoms.

An important ramification of our findings is that in addition to the hollow pentagon, hollow hexagon, and filled hexagon, which are the three motifs considered previously as basic building blocks for large boron cages,[10] it is now necessary to include the pentagon pyramid in the list. The extension to the construction rules for isolated-pentagon cages is straightforward, which amounts to transforming a pair of neighboring pentagon rings to filled pentagons, accompanied by the generation of a pair of adjacent hollow hexagons. An optimal arrangement of those building blocks allows tuning of the aromaticity of the cage, which gives rise to an attractive fluxional behavior and improves the stability.[2,24]

In summary, we have studied a volleyball-shaped B_{80} fullerene that is predicted to be considerably more stable than the previously assumed B_{80} buckyball. Unlike the core-shell-structured $B_{12}@B_{68}$,[17,18] the B_{80} volleyball preserves the ideal electronic analogy to the C_{60} buckyball. The improved stability is shown to be attributed to the rearrangement of capping atoms and the accompanying enhancement in aromaticity. We remark, before closing, that the B_{80} configuration stands for a prototype for understanding the chemical bonding in novel boron nanomaterials. It is worth noting that the isolated hollow-hexagon pair in the B_{80} volleyball is absent in the boron α sheet.[11] In spite of the fact that the boron α sheet is viewed as the counterpart of

graphene and is employed as the precursor for boron nanotubes, it is metallic rather than semimetallic in graphene. Therefore, the capping atom transformation unveiled in the present work may provide useful information in closer scrutiny of the aromaticity in boron sheets. Furthermore, we hope that the advocated stability can promote revived interest in the experimental synthesis. From the perspective of experiments, it is important to understand the building blocks of boron fullerenes. For the B_{80} buckyball and α sheet, the building block is the so-called "snow-drop" fragment.[10] Therefore, the modification of the associated building block as described in this work provides useful guidelines for experimental synthesis.

[1] N. Gonzalez Szwacki, A. Sadrzadeh, and B. I. Yakobson, Phys. Rev. Lett. **98**, 166804 (2007).

[2] W. Huang *et al.*, Nat. Chem. **2**, 202 (2010).

[3] B. Kiran *et al.*, Proc. Natl. Acad. Sci. U.S.A. **102**, 961 (2005).

[4] H. J. Zhai, B. Kiran, J. Li, and L. S. Wang, Nature Mater. **2**, 827 (2003).

[5] H. Kroto, J. Heath, S. O'Brien, R. Curl, and R. Smalley, Nature (London) **318**, 162 (1985).

[6] J. L. Li and G. W. Yang, Appl. Phys. Lett. **95**, 133115 (2009).

[7] A. Y. Liu, R. R. Zope, and M. R. Pederson, Phys. Rev. B **78**, 155422 (2008).

[8] Q. B. Yan, Q. R. Zheng, and G. Su, Phys. Rev. B **80**, 104111 (2009).

[9] Y. F. Zhao *et al.*, Nano Lett. **8**, 157 (2008).

[10] Q. B. Yan, X. L. Sheng, Q. R. Zheng, L. Z. Zhang, and G. Su, Phys. Rev. B **78**, 201401(R) (2008).

[11] H. Tang and S. Ismail-Beigi, Phys. Rev. Lett. **99**, 115501 (2007).

[12] S. Saxena and T. A. Tyson, Phys. Rev. Lett. **104**, 245502 (2010).

[13] N. Gonzalez Szwacki and C. J. Tymczak, Chem. Phys. Lett. **494**, 80 (2010).

[14] A. Sadrzadeh, O. V. Pupysheva, A. K. Singh, and B. I. Yakobson, J. Phys. Chem. A **112**, 13679 (2008).

[15] T. Baruah, M. R. Pederson, and R. R. Zope, Phys. Rev. B **78**, 045408 (2008).

[16] A. Ceulemans, J. T. Muya, G. Gopakumar, and M. T. Nguyen, Chem. Phys. Lett. **461**, 226 (2008).

[17] H. Li *et al.*, Chem. Commun. (Cambridge) **2010**, 3878.

[18] J. Zhao, L. Wang, F. Li, and Z. Chen, J. Phys. Chem. A **114**, 9969 (2010).

[19] A. D. Becke, J. Chem. Phys. **98**, 5648 (1993).

[20] C. Lee, W. Yang, and R. G. Parr, Phys. Rev. B **37**, 785 (1988).

[21] B. Delley, J. Chem. Phys. **92**, 508 (1990); **113**, 7756 (2000).

[22] I. S. Ufimtsev and T. J. Martinez, J. Chem. Theory Comput. **5**, 2619 (2009).

[23] A. Quandt and I. Boustani, ChemPhysChem **6**, 2001 (2005).

[24] N. G. Szwacki, V. Weber, and C. J. Tymczak, Nanoscale Res. Lett. **4**, 1085 (2009).